

Irreducible representations of oscillatory and swirlings flows around microswimmers

Somdeb Ghose¹ and R. Adhikari¹

¹*The Institute of Mathematical Sciences, CIT Campus, Chennai 600113, India*

(Dated: June 12, 2022)

Recent experiments imaging fluid flow around swimming microorganisms have revealed complex time-dependent velocity fields that differ qualitatively from the stresslet flow commonly employed in theory. Here we obtain the most general flow around a finite sized microswimmer by expanding the surface stress in irreducible Cartesian tensors. This expansion, whose first term is stresslet flow, must include third-rank polar and axial tensors to minimally capture crucial features of the oscillatory flow around translating *Chlamydomonas* [Guasto et al., Phys. Rev. Lett., 2010] and the swirling flow around rotating *Volvox* [Drescher et al., Phys. Rev. Lett., 2009] respectively. Axial terms of the expansion produce antisymmetric states of stress, indicating that linear and angular momentum densities are generically coupled in a microswimmer suspension. Macroscopic mean flows can thus be generated in a suspension of spinning particles.

The collective dynamics of microscopic particles that swim in viscous fluids by converting chemical energy to mechanical work is a topic of current interest in non-equilibrium statistical mechanics [1]. Biological and biomimetic examples of such “active” particles include, in increasing order of size, molecular motors [2], active nanobeads [3] and swimming microorganisms. Momentum conservation and the lack of inertia at the microscopic scale implies that the fluid flow around such particles must be both force-free and torque-free, thus constraining it to decay no slower than the inverse square of the distance from the particle. Thus, at distances large compared to the particle size the dominant contribution to the flow is from the dipolar stresslet [4]. Continuum theories, applicable at scales much larger than the particle size, employ the stresslet flow to obtain the long-wavelength, long-time features of the collective dynamics of microswimmer suspensions [5].

However, recent experiments [6] that resolve the flow around swimming microorganisms in unprecedented spatial and temporal detail reveal near field features that cannot be captured by a purely stresslet description. The complex flow around *Chlamydomonas* has easily identifiable qualitative features like stagnation points and strong lateral circulations that vary periodically with time. Both *Chlamydomonas* and *Volvox* rotate about their axis [6] and thus must generate swirling flows while swimming. The flow around a generic translating and rotating microswimmer is then time-dependent with both axisymmetric and swirling components.

The above experiments point to the need of a time-dependent description of microswimming that resolves the finite size of the swimmer and the fluid boundary conditions that prevail on the swimmer surface. These boundary conditions, which may prescribe stresses or velocities, must be able to produce both particle translations and particle rotations. Stresslet flow can do neither and thus it is imperative to identify the minimal set of independent stress modes that can produce a general rigid body motion of the particle. Identifying these

particle stress modes immediately yields the chemomechanical stresses acting on the fluid which are essential for formulating a continuum description of an ensemble of microswimmers.

With these motivations we present, in this Letter, the most general representation of Stokes flow around a finite-sized spherical microswimmer as an expansion in irreducible Cartesian multipoles of the surface stress. The orthogonality and completeness of the tensorial multipoles results provides simple relations between the stresses and velocities that allows us to identify the multipoles necessary and sufficient for translation and rotation. Knowing the rigid body motion we are thus able to reconstruct, using only a few irreducible multipoles, the complex time-dependent flows observed in experiment. The power dissipation and swimming efficiency obtained in terms of these multipoles are in good agreement with experiment. We exploit the rotational invariance manifest in the Cartesian tensor expansion to derive a general constitutive equation for the stress tensor of an active micropolar continuum. In particular, our constitutive equation contains antisymmetric stresses not considered previously. Remarkably, however, these antisymmetric stresses separately conserve orbital and intrinsic angular momenta. We present our method and elaborate on these results below.

Irreducible representations of Stokes flow: Creeping flow around a particle obeys the Stokes equation, $\nabla \cdot \boldsymbol{\sigma} = -\nabla p + \eta \nabla^2 \mathbf{u} = 0$, $\nabla \cdot \mathbf{u} = 0$, where \mathbf{u} is the flow within the volume V , $\boldsymbol{\sigma}$ is the stress, p is the pressure and η is the viscosity. Chemomechanical activity can regulate either the velocity \mathbf{u}^S or the stress $\boldsymbol{\sigma}^S$ on the surface S of the particle, which requires Dirichlet or Neumann boundary conditions, respectively. In either case, the flow in the bulk can be expressed as an integral over the boundary S , where a single layer density $\mathbf{q}(\mathbf{r})$ is convolved with the dyadic Green’s function $\mathbf{G}(\mathbf{r}) = (\mathbb{I} + \hat{\mathbf{r}}\hat{\mathbf{r}})/|\mathbf{r}|^2$ [7]

$$\int_{S'} \mathbf{G}(\mathbf{r} - \mathbf{r}') \cdot \mathbf{q}(\mathbf{r}') dS' = -8\pi\eta \begin{cases} \mathbf{u}(\mathbf{r}), & \mathbf{r} \in V \\ \mathbf{u}^S(\mathbf{r}), & \mathbf{r} \in S, \end{cases} \quad (1)$$

where \mathbf{r} is the field point in the bulk V and \mathbf{r}' is the source point on the surface S . Eq. (1), $\mathbf{r} \in V$, provides a complete solution for the Neumann problem with known single layer density. For the Dirichlet problem, Eq. (1), $\mathbf{r} \in S$, must be solved to obtain the unknown single layer density in terms of the prescribed boundary velocity \mathbf{u}^S .

Lamb provided a general solution of the Stokes equation in terms of three harmonic functions in a spherical harmonic basis [8]. It is convenient to reformulate this solution in a basis of irreducible Cartesian tensors [9] in terms of which succinct and manifestly rotation invariant expressions can be obtained. To this end, we expand the single layer stress density on a sphere of radius a in terms of irreducible Cartesian tensors $\widehat{\mathbf{r}}^{(p)}$, [10]

$$\mathbf{q}(\mathbf{r}) = \sum_{p=0}^{\infty} \frac{(2p+1)!!}{4\pi a^2} \widehat{\mathbf{r}}^{(p)} \odot \mathbf{Q}^{(p+1)}, \mathbf{r} \in S \quad (2)$$

where the multipole moments $Q_{i\alpha_1 \dots \alpha_p}^{(p+1)}$, symmetric and traceless in the last p indices, are given by $p! \mathbf{Q}^{(p+1)} = \int \mathbf{q}(\mathbf{r}) \widehat{\mathbf{r}}^{(p)} dS$. Here \odot indicates a p -fold contraction between a p -th rank tensor and another of higher rank, contracting the last index of the first tensor with the first index of the latter till p indices are contracted, such that $\widehat{\mathbf{r}}^{(p)} \odot \mathbf{Q}^{(p+1)} = \widehat{r}_{\alpha_1 \alpha_2 \dots \alpha_p - 1 \alpha_p} Q_{\alpha_p \alpha_{p-1} \dots \alpha_2 \alpha_1 i}^{(p+1)}$. The $\widehat{\mathbf{r}}^{(p)}$ are symmetric and traceless in every pair of its p indices and obey the orthogonality relation $(2p+1)!! \langle \widehat{\mathbf{r}}^{(p)} \widehat{\mathbf{r}}^{(q)} \rangle = p! \delta_{p,q} \Delta^{(p,p)}$. The surface average $\langle \dots \rangle = (1/4\pi a^2) \int dS$, while the rank $2p$ tensor $\Delta^{(p,p)}$ projects any p -th rank tensor $\widehat{\mathbf{r}}^{(p)}$ to its irreducible form $\widehat{\mathbf{r}}^{(p)}$ [10, 11].

Substituting Eq. (2) into the boundary integral Eq. (1), and following the method detailed in the supplementary information [12], we obtain the solution of the Stokes equation as $\mathbf{u}(\mathbf{r}) = \sum_{p=0}^{\infty} (-1)^{p+1} \mathbf{u}_p(\mathbf{r})$, where

$$\mathbf{u}_p(\mathbf{r}) = a^p \mathbf{Q}^{(p+1)} \odot \nabla(\mathbf{p}) \left(1 + \frac{a^2}{4p+6} \nabla^2 \right) \frac{\mathbf{G}(\mathbf{r})}{8\pi\eta}. \quad (3)$$

The flow \mathbf{u}_p at any order p has contributions which decay as r^{-p} and $r^{-(p+2)}$. Thus the stress multipole expansion automatically generates the Faxén corrections $a^2 \nabla^2 \mathbf{G}(\mathbf{r}) / (4p+6)$ that must be manually reconstructed when expanding in the velocity multipoles of Lamb's general solution [8].

The reducible surface stress multipoles of rank p can be expressed as a direct sum of their irreducible parts, $\mathbf{Q}^{(p)} = \oplus_j \mathbf{Q}^{(p;j)}$ [12], indexed by their weights $j \leq p$. The constraints imposed by incompressibility, biharmonicity and spherical symmetry imply that only a few irreducible parts contribute. Here we focus on the minimal set of multipoles required to produce active translations and rotations. The decompositions we require are [9, 12, 13] $\mathbf{Q}^{(1)} = \mathbf{F}$, $a \mathbf{Q}^{(2)} = \mathbf{S} - \frac{1}{2} \epsilon \cdot \mathbf{T}$, $a^2 \mathbf{Q}^{(3)} = \mathbf{\Gamma}_{i\alpha\beta} + \frac{2}{3} \{ \epsilon \cdot \Psi + (\epsilon \cdot \Psi)^T \}_{i\alpha\beta} + \frac{1}{10} (-2\mathbf{d}_i \mathbb{I}_{\alpha\beta} + 3\mathbf{d}_\alpha \mathbb{I}_{\beta i} + 3\mathbf{d}_\beta \mathbb{I}_{i\alpha})$,

$a^3 \mathbf{Q}^{(4;3)} = -\frac{3}{4} \widehat{\epsilon \cdot \Lambda}$ where $\widehat{\dots}$ denotes complete symmetrization and ϵ is the rank-3 antisymmetric Levi-Civita tensor. The force \mathbf{F} , the torque \mathbf{T} , stresslet \mathbf{S} and the potential dipole \mathbf{d} are familiar irreducible multipoles. The new irreducible multipoles introduced here are the second rank pseudodeviatoric torque dipole Ψ or the “vortlet”, the third rank septorial stresslet dipole $\mathbf{\Gamma}$ or the “septlet”, and the third rank pseudoseptorial multipole Λ or the “spinlet”. Using these decompositions and Eq. (3), force-free torque-free flows decaying no faster than r^{-5} are expressed as

$$\begin{aligned} 8\pi\eta \mathbf{u}^a(\mathbf{r}) = & \left(1 + \frac{a^2}{10} \nabla^2 \right) \nabla \mathbf{G} \odot \mathbf{S} + \frac{1}{5} \nabla^2 \mathbf{G} \cdot \mathbf{d} \\ & + \frac{4}{3} (\Psi \cdot \nabla) \cdot (\nabla \times \mathbf{G}) - \left(1 + \frac{a^2}{14} \nabla^2 \right) \nabla \nabla \mathbf{G} \odot \mathbf{\Gamma} \\ & - \frac{3}{4} (\Lambda : \nabla \nabla) \cdot (\nabla \times \mathbf{G}). \end{aligned} \quad (4)$$

The total number of independent coefficients is 27 with the individual multipoles above contributing 5, 3, 5, 7 and 7 independent coefficients respectively. The stresslet \mathbf{S} completely characterizes active flows decaying as r^{-2} . The potential dipole \mathbf{d} , the vortlet Ψ and the septlet $\mathbf{\Gamma}$ together completely characterize flows decaying as r^{-3} . The spinlet Λ produces a flow decaying as r^{-4} . The vortlet and the spinlet produce swirling flows which have not been considered before. Flows due to the first four multipoles are plotted in [12], while the spinlet flow is plotted in Fig. (3).

Active particle motion : The active translations \mathbf{V} and rotations Ω of the *particle* can be obtained from the linear relation between the velocity and stress multipoles at the boundary, where $\mathbf{u}^S(\mathbf{r}) = \mathbf{V} + a\Omega \times \widehat{\mathbf{r}} + \mathbf{v}^a(\mathbf{r})$ and \mathbf{v}^a is an activity induced surface velocity. Expanding the surface velocity $\mathbf{u}^S(\mathbf{r})$ in the same irreducible basis $\widehat{\mathbf{r}}^{(p)}$ and using Eq. (1), $\mathbf{r} \in S$, the linear relationships can be expressed explicitly as [12]

$$\mathbf{F} = -6\pi\eta a (\mathbf{V} + \langle \mathbf{v}^a \rangle) \quad (5a)$$

$$\mathbf{T} = -8\pi\eta a^2 \left(a\Omega - \frac{3}{2} \langle \mathbf{v}^a \times \widehat{\mathbf{r}} \rangle \right) \quad (5b)$$

$$\mathbf{S} = -10\pi\eta a^2 \langle \mathbf{v}^a \widehat{\mathbf{r}} + (\mathbf{v}^a \widehat{\mathbf{r}})^T \rangle \quad (5c)$$

$$\mathbf{d} = -30\pi\eta a^3 \left\langle (\mathbf{v}^a \cdot \widehat{\mathbf{r}}) \widehat{\mathbf{r}} - \frac{1}{3} \mathbf{v}^a \right\rangle \quad (5d)$$

$$\Psi = 5\pi\eta a^3 \left\langle (\mathbf{v}^a \times \widehat{\mathbf{r}}) \widehat{\mathbf{r}} + \{ (\mathbf{v}^a \times \widehat{\mathbf{r}}) \widehat{\mathbf{r}} \}^T \right\rangle \quad (5e)$$

$$\mathbf{\Gamma} = -\frac{35}{2} \pi\eta a^3 \left\langle \widehat{\mathbf{v}^a \widehat{\mathbf{r}}} - \frac{2}{5} (\mathbf{v}^a \cdot \widehat{\mathbf{r}}) \widehat{\mathbf{r}} \mathbb{I} - \frac{1}{5} \mathbf{v}^a \mathbb{I} \right\rangle \quad (5f)$$

$$\Lambda = 14\pi\eta a^4 \left\langle \widehat{(\mathbf{v}^a \times \widehat{\mathbf{r}}) \widehat{\mathbf{r}}} - \frac{3}{5} \widehat{(\mathbf{v}^a \times \widehat{\mathbf{r}}) \mathbb{I}} \right\rangle. \quad (5g)$$

The first two relations above show that a force-free torque-free particle acquires translation and rotational motion only if the surface averages of the \mathbf{v}^a and $\mathbf{v}^a \times \widehat{\mathbf{r}}$

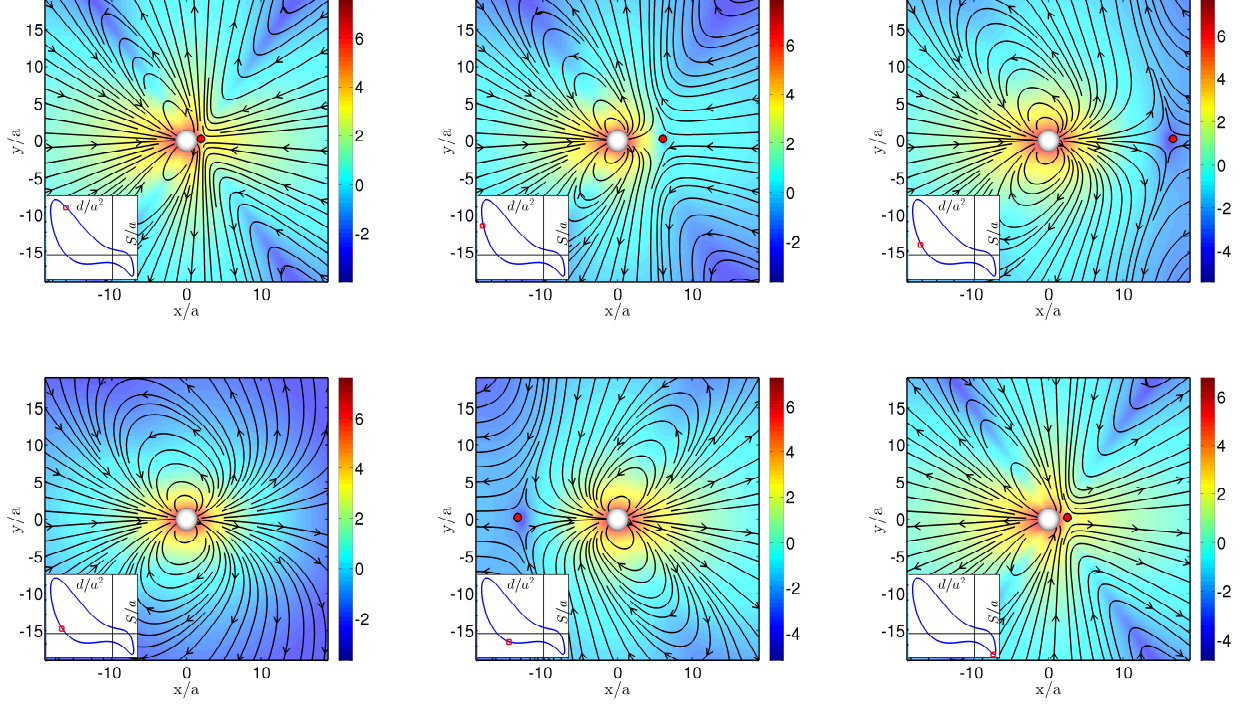


FIG. 1. (Color) Cross-sections of complex and time-dependent long-range hydrodynamic flows around a spherical active particle of radius a generated by a simple linear combination of time-dependent stresslet \mathbf{S} , potential dipole \mathbf{d} and septlet $\mathbf{\Gamma}$. Streamlines show the direction of the flow while the background color represents the natural logarithm of the strength of the flow. The red dot indicates the approximate position of the stagnation point. These flow fields capture the essential features of experimentally measured flow fields around a swimming *Chlamydomonas* [6]. The inset shows the variation of the potential dipole and the stresslet; the blue line shows the overall variation, while the red square shows the values for the current frame.

are non-zero [14]. The remaining relations appear to be new. The utility of these relations is that, given the active \mathbf{V} and $\mathbf{\Omega}$, they determine the minimal external flow $\mathbf{u}^a(\mathbf{r})$. This $\mathbf{u}^a(\mathbf{r})$ is the sum of a potential dipole of strength $\mathbf{d} = -30\pi\eta a^3 [\langle (\mathbf{v}^a \cdot \hat{\mathbf{r}}) \hat{\mathbf{r}} \rangle + \frac{1}{3}\mathbf{V}]$ and a spinlet

of strength $\mathbf{\Lambda} = 14\pi\eta a^4 [\langle (\mathbf{v}^a \times \hat{\mathbf{r}}) \hat{\mathbf{r}} \hat{\mathbf{r}} \rangle - \frac{2a}{5}\mathbf{\Omega} \mathbb{I}]$. The stresslet \mathbf{S} , the septlet $\mathbf{\Gamma}$ and the vortlet $\mathbf{\Psi}$ modify the external flow without affecting \mathbf{V} and $\mathbf{\Omega}$. However, they contribute to long range flows and, thus, influence inter-particle hydrodynamic interactions. Eq. (5) provides a manifestly rotational invariant relationship between the external flow and the rigid body motion, \mathbf{V} and $\mathbf{\Omega}$, and active surface velocity \mathbf{v}^a of the particle. Previous work only considered the relationship between rigid body motion and surface velocity confined to purely antisymmetric flows, thus missing the crucial active swirling flow components considered here.

Using Eq. (2) and the linear relation between the stress and velocity multipoles, the power dissipated into the fluid, $\dot{W} = -\int \mathbf{q} \cdot \mathbf{u}^S dS$, is obtained in terms of the

multipole moments of the stress as

$$\dot{W} = -\sum_{p=0}^{\infty} \mathbf{Q}^{(p+1)} \odot \mathcal{G}^{(p+1, p+1)} \odot \mathbf{Q}^{(p+1)}, \quad (6)$$

where the matrix \mathcal{G} is diagonal in rank and weight (see [12]). Resolving into irreducible parts gives

$$\begin{aligned} \dot{W} = & \frac{3}{20\pi\eta a^3} \mathbf{S} \odot \mathbf{S} + \frac{3}{10\pi\eta a^5} \mathbf{d} \odot \mathbf{d} + \frac{32}{3\pi\eta a^5} \mathbf{\Psi} \odot \mathbf{\Psi} \\ & + \frac{6}{7\pi\eta a^5} \mathbf{\Gamma} \odot \mathbf{\Gamma} + \frac{675}{16\pi\eta a^7} \mathbf{\Lambda} \odot \mathbf{\Lambda}. \end{aligned} \quad (7)$$

We use Eqs. (4), (5) and the relations for the dissipated power to analyze the time-dependent oscillatory motion of *Chlamydomonas* that produces long range approximately axisymmetric flow and the rotational motion of *Volvox* that produces a short range swirling flow.

Oscillatory flows: The flow around the microorganism *Chlamydomonas reinhardtii* has recently been measured in detail to reveal a flow field that is “complex and highly time-dependent” [6]. We are able to capture the essential features of this flow by superposing flows due to the potential dipole, stresslet, and septlet with time-varying

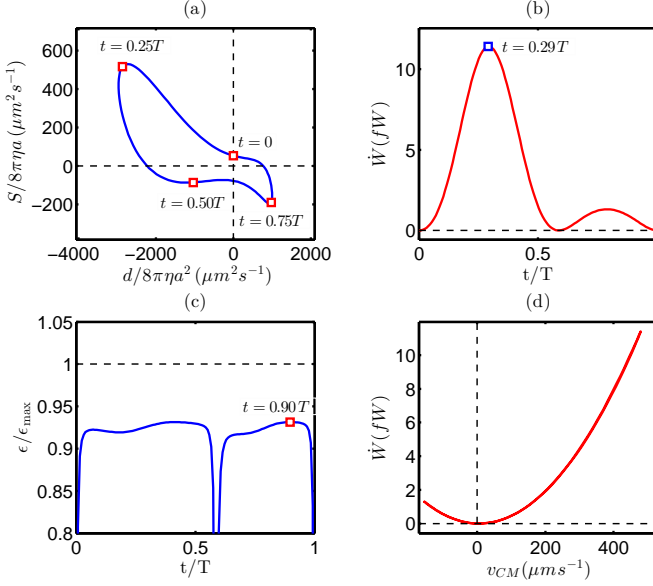


FIG. 2. (Color) Power dissipation and swimming efficiency of *Chlamydomonas*, computed using a linear combination of a stresslet \mathbf{S} , a potential dipole \mathbf{d} and a septlet $\mathbf{\Gamma}$. Panel (a) shows the variation of the strength of the potential dipole against the stresslet strength, the former estimated from particle image velocimetry data of *Chlamydomonas* swimming [6]. Panel (b) shows the time variation of the dissipated power, while (d) shows the variation of the power against the translational velocity. The relative efficiency is maximum near the middle and end of the cycle, panel (c).

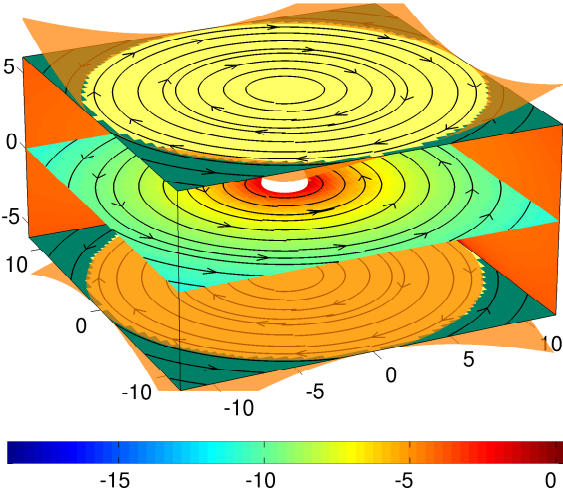


FIG. 3. (Color) Swirling flows around an actively rotating particle of radius a generated by a uniaxially parametrized spinlet $\mathbf{\Lambda}$, Eq. (4). Streamlines show the direction of the flow while the background color represents the natural logarithm of the strength of the flow. The spinlet produces r^{-4} flows that rotate in the same direction at the particle surface but switch directions across the isosurface $\cos^2 \theta = 1/5$, where θ is the polar angle. We predict this to represent swirling flows around *Volvox*.

strengths. Assuming particle motion to occur along the y -axis the multipoles are parametrized uniaxially as $\mathbf{S} = S_0(t)(\hat{\mathbf{y}}\hat{\mathbf{y}} - \frac{1}{3}\mathbb{I})$, $\mathbf{d} = d_0(t)\hat{\mathbf{y}}$ and $\mathbf{\Gamma} = \Gamma_0(t)(\hat{\mathbf{y}}\hat{\mathbf{y}}\hat{\mathbf{y}} - \frac{3}{5}\hat{\mathbf{y}}\mathbb{I})$. The data of [6] shows that the translation speed can be very well parametrized by the first two Fourier modes, $V(t) = (a_0/2)[1 + (2a_1/a_0)\cos(\omega t) + (2a_2/a_0)\cos(2\omega t) + (2b_1/a_0)\sin(\omega t) + (2b_2/a_0)\sin(2\omega t)]$, where a_0 is in units of $\mu\text{m s}^{-1}$ (see [12]). This yields, through Eq. (5a) and (5d), $d_0(t) = -10\pi\eta a^3 V(t)$. $S_0(t)$ and $\Gamma_0(t)$ are then determined by the position of the stagnation point relative to the center of the particle. The flow fields produced by this analysis are shown at selected times of the cycle in Fig. (1) and in the supplementary video [12]. They are in good agreement with the corresponding figures in [6].

The time variation of $d_0(t)$ and $S_0(t)$ can be plotted as an orbit in the (d_0, S_0) plane, as shown in Fig. (2a). The stagnation point is ahead of the particle when the orbit is in the second and fourth quadrants, $d_0 S_0 < 0$, while it is behind the particle when the orbit is in the first or third quadrants, $d_0 S_0 > 0$. The particle moves forward (backward) when the orbit is in the left (right) half plane. The instantaneous power dissipation is plotted in Fig. (2b). On average, a *Chlamydomonas* of size $3.5 \mu\text{m}$ swimming at $134 \mu\text{m s}^{-1}$ in water at 20°C dissipates approximately 6 fW of power. Both the instantaneous power variation and the average power values are in good agreement with experimental findings [6]. The instantaneous efficiency of translation, defined as ratio of power expended by an external force to maintain a rigid sphere in uniform motion with speed V to that expended chemomechanically to maintain the same speed [15], $\epsilon(t) = 6\pi\eta a V^2 / \dot{W}(t)$, is plotted in Fig. (2c). The efficiency is maximum towards the middle and end of the cycle, with the maximum value being close to the theoretical maximum of 20% (see [12]). The power dissipation as a function of the speed, shown in Fig. (2d), shows the expected quadratic dependence.

Swirling flows: Like most microorganisms, *Volvox carteri* rotates around its own axis as it swims. Using the minimal representation for the spinlet strength, $\Lambda_0 = -(28/5)\pi\eta a^5 \Omega$, and parametrizing uniaxially, $\mathbf{\Lambda} = \Lambda_0(t)(\hat{\mathbf{y}}\hat{\mathbf{y}}\hat{\mathbf{y}} - \frac{3}{5}\hat{\mathbf{y}}\mathbb{I})$, we are able to capture the short-ranged swirling flow field responsible for self-rotation, Fig. (3). Swirling flows due to the vortlet do not contribute to *Volvox* rotation since they produce swirling flows that spin in opposite directions on the particle surface and thus cancel out (see supplementary Fig. (S2) [12]). Rotation induced by spinlet swirling flows have a maximum swimming efficiency of 1.5% in the Lighthill sense [15]. Representing the *Volvox* by a uniaxial spinlet whose strength has been computed using its minimal representation, we calculate the rotational power dissipated by a *Volvox* of size $150 \mu\text{m}$ rotating at 1 rad s^{-1} in water at 20°C to be approximately 250 fW. Swirling flows around *Volvox*, if experimentally measured, can shed light on the swimming mechanism that must pro-

duce the antisymmetric velocity moments on the particle surface.

Active stress densities: Continuum hydrodynamic descriptions of active matter with stresses of the form $\boldsymbol{\sigma} = -p\mathbb{I} + \eta[\nabla\mathbf{u} + (\nabla\mathbf{u})^T] + \boldsymbol{\sigma}^a$ were first proposed in [16]. The active stress $\boldsymbol{\sigma}^a$ can do work on the fluid and increase the fluid kinetic energy only if the solenoidal part of the divergence of the active stress is nonzero [16]. Since $-\nabla p + \eta\nabla^2\mathbf{u} = \nabla \cdot \boldsymbol{\sigma}^a$, contributions to the active stress from each irreducible multipole can be identified from the coefficient of the Green's function in Eq. (3). For the multipoles presented in Eq. (4) the result is

$$\boldsymbol{\sigma}^s(\mathbf{r}) = \left(1 + \frac{a^2\nabla^2}{10}\right)\mathbf{S} + \frac{2}{5}\widehat{\nabla\mathbf{d}} - \left(1 + \frac{a^2\nabla^2}{14}\right)\nabla \cdot \boldsymbol{\Gamma} \quad (8a)$$

$$\mathbf{A}(\mathbf{r}) = \frac{4}{3}\left(1 + \frac{a^2\nabla^2}{14}\right)\nabla \cdot \boldsymbol{\Psi} - \frac{3}{4}\left(1 + \frac{a^2\nabla^2}{18}\right)\nabla\nabla : \boldsymbol{\Lambda} \quad (8b)$$

where the active stress is written in terms of its symmetric and antisymmetric parts, $\boldsymbol{\sigma}^a = \boldsymbol{\sigma}^s + \boldsymbol{\epsilon} \cdot \mathbf{A}$. Tensorial densities are now defined for a suspension of N particles located at \mathbf{r}_n as $\mathbf{S}(\mathbf{r}) = \sum_n \mathbf{S}_n \delta(\mathbf{r} - \mathbf{r}_n)$ and similarly for the remaining multipoles.

Symmetric states of active stress have been considered previously in the literature in the $a \rightarrow 0$ limit and for uniaxial stresslets and the potential dipole. Our derivation shows that stresslet contribution includes a finite size correction and is generally biaxial. The septlet, not considered previously, contributes at the same order in gradients as the potential dipole and produces a long range r^{-3} flow. Thus, it is of equal importance as the potential dipole for collective hydrodynamics.

Antisymmetric states of active stress, to the best of knowledge, have not been considered in the literature before. Angular momentum conservation dictates that such states of stress can exist only when the medium has an internal “spin” angular momentum \mathbf{l} over and above the orbital angular momentum $\mathbf{r} \times \mathbf{u}$. Antisymmetric stresses couple orbital and spin angular momentum through the pair of conservation equations $\partial_t(\mathbf{r} \times \mathbf{g}) + \nabla \cdot (\mathbf{r} \times \mathbf{g}\mathbf{v}) = \nabla \cdot (\mathbf{r} \times \boldsymbol{\sigma}^s) - \mathbf{A}$, $\partial_t\mathbf{l} + \nabla \cdot (\mathbf{l}\mathbf{u}) = \nabla \cdot \mathbf{c} + \mathbf{A}$, where \mathbf{c} is the couple stress [17]. Remarkably, and in distinction with antisymmetric states of stress in polyatomic liquids, the antisymmetric active stress \mathbf{A} is a divergence, Eq. (8b). Thus local transfers between orbital and spin angular momentum are allowed but their global values remain unchanged. Antisymmetric states of stress also couple the linear momentum \mathbf{g} to the angular momenta through $\partial_t\mathbf{g} + \nabla \cdot (\mathbf{g}\mathbf{u}) = \nabla \cdot \boldsymbol{\sigma}^s + \frac{1}{2}\nabla \times \mathbf{A}$ [17]. This implies that self-rotating particles, through their hydrodynamic interaction, can set up spontaneous macroscopic flows in suspension. This is macroscopic manifestation of the translational velocity $(1 + a^2\nabla^2/6)\mathbf{u}^{(A)}$ of a passive particle at \mathbf{r} induced by a spinlet at the origin.

Self-rotating particles with spinlets and/or particles with septlets produce continuum stresses described by third rank tensorial densities. Thus, third-rank orientational order parameters must be introduced to better describe spinning active micropolar continua, going beyond the second-rank tensorial descriptions of [5]. For swimming microorganisms like *Chlamydomonas* generating time-varying flows, the stress multipoles appearing in Eq. (8) are time-dependent, and so is $\boldsymbol{\sigma}^a$. In a collection of such active particles, the phase of the stress tensor thus depends on the relative locations of individual particles. The synchronisation of phases by many-body hydrodynamic interactions can be studied using a generalization to N particles of the approach presented here.

Discussion: The close agreement of our results for the flow field, power dissipation, and efficiencies with those of [6] shows the efficacy of our minimal irreducible multipole expansion for studying complex time-dependent flows around active particles. This expansion forms the basis of a method to obtain many-body hydrodynamic interactions in a suspension of finite-sized microswimmers. The method can be used to obtain the rheology of a microswimmer suspension including hydrodynamic interactions to second order in volume fraction. We urge the experimental verification of the swirling flows around rotating microswimmers, the separate conservation of orbital and angular momentum, and the macroscopic flows generated in a suspension of spinning particles.

Financial support from PRISM II, Department of Atomic Energy, Government of India is gratefully acknowledged. We thank G. Baskaran, M. E. Cates, G. Date, R. E. Goldstein, A. J. C. Ladd, M. Polin, R. Simon, H. A. Stone and P. B. Sunil Kumar for helpful discussions. We thank R. E. Goldstein and M. Polin for kindly sharing their data of [6] and answering our queries, and A. J. C. Ladd for generously sharing his personal notes as well as for many useful suggestions.

-
- [1] T. Pedley and J. Kessler, *Annu. Rev. Fluid Mech.* **24**, 313 (1992); L. H. Cisneros, R. Cortez, C. Dombrowski, R. E. Goldstein, and J. O. Kessler, *Exp. Fluids* **43**, 737 (2007); E. Lauga and T. Powers, *Rep. Prog. Phys.* **72**, 096601 (2009); S. Ramaswamy, *Annu. Rev. Condens. Mat. Phys.* **1**, 323 (2010); M. Cates and F. MacKintosh, *Soft Matter* **7**, 3050 (2011); D. L. Koch and G. Subramanian, *ibid.* **43**, 637 (2011); E. Lauga and R. Goldstein, *Phys. Today* **65**, 30 (2012); M. C. Marchetti, J. F. Joanny, S. Ramaswamy, T. B. Liverpool, J. Prost, M. Rao, and R. A. Simha, *Rev. Mod. Phys.* **85**, 1143 (2013).
 - [2] F. J. Nédélec, T. Surrey, A. C. Maggs, and S. Leibler, *Nature* **389**, 305 (1997).
 - [3] W. F. Paxton, K. C. Kistler, C. C. Olmeda, A. Sen, S. K. S. Angelo, Y. Cao, T. E. Mallouk, P. E. Lammert, and V. H. Crespi, *J. Am. Chem. Soc.* **126**, 13424 (2004); J. Vicario, R. Eelkema, W. R. Browne, A. Meetsma,

- R. M. La Crois, and B. L. Feringa, *Chem. Commun.* **31**, 3936 (2005); J. M. Catchmark, S. Subramanian, and A. Sen, *Small* **1**, 202 (2005); G. A. Ozin, I. Manners, S. Fournier-Bidoz, and A. Arsenault, *Adv. Mater.* **17**, 3011 (2005).
- [4] G. Batchelor, *J. Fluid Mech.* **41**, 545 (1970).
- [5] R. A. Simha and S. Ramaswamy, *Phys. Rev. Lett.* **89**, 058101 (2002); D. Saintillan and M. J. Shelley, *Phys. Rev. Lett.* **100**, 178103 (2008).
- [6] K. Drescher, K. C. Leptos, I. Tuval, T. Ishikawa, T. J. Pedley, and R. E. Goldstein, *Phys. Rev. Lett.* **102**, 168101 (2009); J. S. Guasto, K. A. Johnson, and J. P. Gollub, *Phys. Rev. Lett.* **105**, 168102 (2010); K. Drescher, R. Goldstein, N. Michel, M. Polin, and I. Tuval, *Phys. Rev. Lett.* **105**, 168101 (2010).
- [7] O. Ladyzhenskaia, *The mathematical theory of viscous incompressible flow*, Mathematics and its applications (Gordon and Breach, 1969); C. Pozrikidis, *Boundary Integral and Singularity Methods for Linearized Viscous Flow* (Cambridge University Press, Cambridge, 1992); S. Kim and S. Karrila, *Microhydrodynamics: Principles and Selected Applications*, Dover Civil and Mechanical Engineering Series (Dover Publications, 2005).
- [8] H. Lamb, *Hydrodynamics* (University Press, 1916).
- [9] J. Coope, R. Snider, and F. McCourt, *J. Chem. Phys.* **43**, 2269 (1965); J. Jerphagnon, *Phys. Rev. B* **2**, 1091 (1970); J. Jerphagnon, D. Chemla, and R. Bonneville, *Adv. Phys.* **27**, 609 (1978).
- [10] P. Mazur and W. Van Saarloos, *Physica A: Stat. Mech. Appl.* **115**, 21 (1982); A. J. Ladd, *J. Chem. Phys.* **88**, 5051 (1988).
- [11] S. Hess and W. Köhler, *Formeln zur tensor-rechnung* (Palm & Enke, 1980).
- [12] “See Supplemental Material at [URL will be inserted by publisher] for detailed calculations, plots of flow fields and a movie showing the reconstruction of the complex time-dependent flow around *Chlamydomonas*.”
- [13] D. Andrews and W. Ghoul, *Phys. Rev. A* **25**, 2647 (1982).
- [14] H. Brenner, *Chem. Engg. Sci.* **18**, 1 (1963); J. Anderson and D. Prieve, *Langmuir* **7**, 403 (1991); H. A. Stone and A. D. T. Samuel, *Phys. Rev. Lett.* **77**, 4102 (1996).
- [15] M. J. Lighthill, *Commun. Pure. Appl. Math.* **5**, 109 (1952).
- [16] B. Finlayson and L. Scriven, *Proc. Roy. Soc. A* **310**, 183 (1969).
- [17] J. S. Dahler, *The Journal of Chemical Physics* **30**, 1447 (1959).